Autodetachment study of the electronic spectroscopy of FeO−

T. Andersen, K. R. Lykke, D. M. Neumark, and W. C. Lineberger

Citation: The Journal of Chemical Physics **86**, 1858 (1987); doi: 10.1063/1.452137
View online: http://dx.doi.org/10.1063/1.452137
View Table of Contents: http://scitation.aip.org/content/aip/journal/jcp/86/4?ver=pdfcov
Published by the AIP Publishing

Autodetachment study of the electronic spectroscopy of FeO^-

T. Andersen,[a] K. R. Lykke, D. M. Neumark,[b] and W. C. Lineberger
Joint Institute for Laboratory Astrophysics, University of Colorado and National Bureau of Standards and Department of Chemistry and Biochemistry, University of Colorado, Boulder, Colorado 80309

(Received 8 July 1986; accepted 27 October 1986)

The anion FeO^- was studied by autodetachment spectroscopy in a coaxial laser–ion beam photodetachment spectrometer. Transitions were observed between the ground electronic state of the ion and several excited electronic states near the electron detachment threshold. Rotational assignments were carried out for several bands, and the measured linewidths yielded autodetachment lifetimes as a function of rotational energy for these bands. The results indicate a $^4\Delta$ ground state of FeO^-. The autodetachment lifetimes show that some of the excited electronic states are dipole bound, and that one weakly bound state may be a valence excited state.

I. INTRODUCTION

Molecular negative ions have become an inviting target[1–5] for the techniques of high resolution spectroscopy developed in recent years. The combination of autodetachment and absorption experiments will lead to a new level in our understanding of the structure of these species. The electronic structure of negative ions is particularly interesting because the typically low electron binding energies are expected to result in orbitals that are quite different from the highest occupied molecular orbitals in neutral species. High resolution electronic spectroscopy of negative ions provides an excellent probe of electronic structure and its relationship to the vibrational and rotational degrees of freedom. However, while nearly all molecular negative ions have a discrete vibrational spectrum,[1,2] the range of ions that can be studied by electronic spectroscopy is more limited, because most known negative ions do not have bound or long-lived excited electronic states. The reason for this is that for most anions, the first excited electronic state lies well above the threshold for electron detachment, and autodetachment is expected to occur sufficiently rapidly to obliterate any sharp spectral structure in transitions between the ground and excited electronic states. Moreover, negative ions do not have Rydberg states since the molecular core is neutral. Thus, high resolution electronic spectroscopy of negative ions is limited to those ions with electronic states lying below or just above the detachment threshold.

For many years, C_2^- was the only negative ion known to have a bound, excited electronic state.[3] This is a valence state that occurs because of low-lying excited molecular orbital configurations in C_2^-. More recently, dipole-bound electronic states have been observed in negative ions.[4,5] These states occur near the electron detachment threshold in anions for which the dipole moment of the neutral molecular core is greater than ~ 2 D and are, in a sense, the negative ion analogs of Rydberg states. Theoretical studies[6–8] of the properties of dipole-bound states predict that the orbital for the dipole-bound electron is exceedingly diffuse, typically extending well over 10 Å. The system reported here, FeO^-, may well have both valence and dipole-bound excited electronic states near the detachment threshold, and one of the issues addressed here is whether one can unambiguously label the type of electronic state based on an experimental observable.

The choice of FeO^- was motivated by two factors. It was predicted[9] to have a sufficiently large dipole moment to support a dipole-bound state. In addition, from the previously determined[10] electron affinity of FeO, 12 040 cm^{-1}, the FeO^- photodetachment threshold was known to be within the frequency range of cw single mode tunable dye lasers. Our primary interest was to study dipole-bound states in a diatomic molecule and to contrast their behavior to dipole-bound states in the acetaldehyde enolate anion[4] $C_2H_3O^-$. Since neutral transition metal oxides are known to have numerous low-lying electronic states,[11,12] the possibility also existed that FeO^- would have excited valence states near its detachment threshold. The FeO^- anion thus presented the unique opportunity to study both types of electronic states simultaneously.

The method used to study FeO^-, tunable laser autodetachment spectroscopy, has been described in detail previously.[4,13] This high resolution (~ 20 MHz) technique requires the existence of long-lived vibrationally or electronically excited states of the ion that lie just above the detachment threshold. In the case of FeO^-, transitions between the ground and various excited electronic states above the electron detachment threshold are accessed with a tunable laser, and the excited states decay by autodetachment to neutral FeO plus an electron, both of which are subsequently detected with high efficiency. As the laser frequency is scanned, these transitions to autodetaching states appear as sharp resonances on a relatively smooth background arising from direct photodetachment. The spectrum of the autodetachment resonances is similar, although not identical, to the absorption spectrum above the detachment threshold of the negative ion, and the resolved (Lorentzian) resonance widths yield the lifetime of the autodetaching state. Thus, from a single experiment we learn about the spectroscopy and autodetachment dynamics of FeO^-.

The autodetachment spectrum of FeO^- consists of transitions to several electronic states, but only a few bands

[a] 1984–85 JILA Visiting Fellow. Permanent address: Institute of Physics, University of Aarhus, Denmark.
[b] Permanent address: Department of Chemistry, University of California, Berkeley, California 94720.

 0021-9606/87/041858-10$02.10

have been fully rotationally assigned. The complexity of the spectrum is not surprising in light of the fact that the neutral FeO electronic absorption spectrum[11] is extremely congested and perturbed. The ground state of FeO is $^5\Delta$ and that for FeO^- has been predicted[14] to be $^4\Delta$, a prediction supported by our results. The nature of the excited states are revealed more by the resonance linewidth results than by the line positions. The autodetachment rate dependence on the rotational state of the ion is quite different for different bands in the spectrum, and this allows one to distinguish, to some extent, between dipole-bound and valence autodetaching states. A preliminary account of this work has recently been reported.[15]

II. EXPERIMENTAL

The coaxial beam photodetachment apparatus and the laser system used in this study have been described in detail before[4,13] and will be discussed only briefly. A 0.1 nA beam of FeO^- ions is extracted from a low pressure electric discharge ion source in which iron pentacarbonyl is burned with N_2O. The ion beam is mass analyzed, accelerated to 3.2 keV, and injected into the ultrahigh vacuum part of the detachment apparatus (pressure $\sim 4\times 10^{-9}$ Torr) in which it is merged with the laser beam over a 30 cm path with an electrostatic quadrupole deflector. The electrons generated by photodetachment are extracted from the interaction region with a weak magnetic field, and are detected by a ceramic electron multiplier. After leaving the interaction region, the remaining negative ions are separated from the neutrals formed by photodetachment by a second quadrupole deflector. The 3.2 keV neutrals strike a KDP crystal, producing secondary electrons, which are detected by a second ceramic electron multiplier.

The laser system used is identical to the one applied to the study of O^- photodetachment.[16] All experiments were carried out in the 11 500–12 900 cm^{-1} region with the dyes styryl 9 or 8, pumped with up to 7 W of light from an argon-ion laser operating on all lines. Broadband output was roughly 400 mW at the peak of the gain curve; single mode output was 150–200 mW. With the laser operating in its single-mode configuration, the overall spectral resolution was limited to ~ 20 MHz by the residual Doppler width of the fast ion beam, based on the width of the most narrow lines observed. Typical signal rates were $\sim 10\,000$ counts/s, and single-mode scans of ~ 0.5 cm^{-1} were completed in ~ 5 min.

The line shape of the laser was monitored by two Fabry–Perot étalons. Absolute wavelength calibration to an accuracy of ± 0.003 cm^{-1} was provided by a lambda meter[17] of the traveling Michelson interferometer type using a polarization-stabilized helium–neon laser reference.[18] The photoabsorption data presented here have been corrected for the first-order Doppler shift, approximately 4 cm^{-1} for the frequency range used.

III. RESULTS

Figure 1 shows an autodetachment spectrum of FeO^- taken with the laser in its broadband configuration with 1 cm^{-1} resolution. The spectrum consists of autodetachment features superimposed on a direct photodetachment background that increases with photon energy. In the absence of autodetachment, this spectrum would show several thresholds[16] resulting from transitions between various spin orbit levels of FeO^- and FeO. However, the autodetachment structure is sufficiently intense to obscure these direct photodetachment thresholds.

Most of the autodetachment structure in Fig. 1 is not rotationally resolved at 1 cm^{-1} (30 GHz) resolution; the one exception is the band ranging from 11 820–11 920 cm^{-1}, labeled band I in the figure. With the laser operating in its medium-resolution ($\Delta\nu \cong 1$ GHz) configuration, band I was clearly resolved, as was another band extending from 12 060–12 110 cm^{-1}, labeled band II in Fig. 1. In addition, considerable autodetachment structure was observed between 11 700 and 12 100 cm^{-1} in which the true linewidths were not resolved. Most of this region was therefore also scanned with the laser operating in a single mode, at an effective resolution of $\lesssim 20$ MHz. This high resolution scan revealed many more band systems, of which only three could be rotationally assigned. These bands are designated

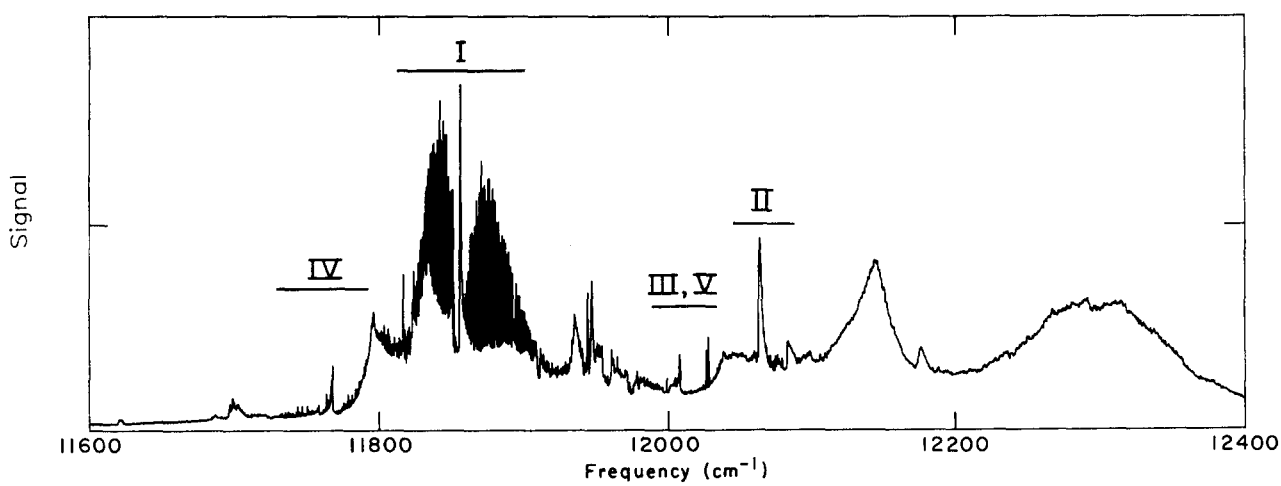

FIG. 1. Low resolution scan (~ 1 cm^{-1}) of the photodetachment spectrum of FeO^-. The locations of bands I–V are indicated.

TABLE I. Assigned rotational lines for FeO^-. Upper (lower) components for bands IV and V correspond to energy levels given by Eq. (3) [Eq. (4)] in the text. All line positions are in cm^{-1} and have been corrected for the Doppler shift.

	P		*Q*		*R*	
J''	Obs.	Obs. − Calc.	Obs.	Obs. − Calc.	Obs.	Obs. − Calc.
			Band I			
2.5					11 863.410	0.000
3.5	11 856.386	0.005			11 864.453	0.002
4.5	11 855.414	0.000			11 865.513	0.011
5.5	11 854.446	− 0.010			11 866.557	− 0.004
6.5	11 853.513	0.005			11 867.632	0.002
7.5	11 852.576	0.007			11 868.690	− 0.017
8.5	11 851.634	− 0.005			11 869.789	− 0.004
9.5	11 850.717	− 0.002			11 870.901	0.013
10.5	11 849.804	− 0.004			11 871.993	0.002
11.5	11 848.898	− 0.007			11 873.093	− 0.009
12.5	11 848.009	− 0.003			11 874.229	0.007
13.5	11 847.137	0.010			11 875.351	0.001
14.5	11 846.252	0.000			11 876.481	− 0.005
15.5	11 845.387	0.002			11 877.627	− 0.002
16.6	11 844.540	0.014			11 878.784	0.004
17.5	11 843.663	− 0.013			11 879.938	0.000
			Band II			
3.5	12 082.639	− 0.002	12 086.160	− 0.010		
4.5	12 081.694	− 0.004	12 086.239	0.004		
5.5	12 080.778	0.010	12 086.313	− 0.001		
6.5	12 079.853	− 0.001	12 086.410	0.002		
7.5	12 078.962	0.009	12 086.521	0.004		
8.5	12 078.066	− 0.002	12 086.642	0.002		
9.5	12 077.184	− 0.012	12 086.776	− 0.002		
10.5	12 076.341	0.002	12 086.931	0.000		
11.5	12 075.491	− 0.005	12 087.094	− 0.005		
12.5	12 074.675	0.007	12 087.283	0.002		
			Band III			
13.5					12 027.118	0.004
14.5					12 028.288	− 0.006
15.5	11 997.303	− 0.001			12 029.479	0.000
16.5	11 996.500	0.001			12 030.671	0.002
17.5	11 995.701	0.000			12 031.862	− 0.001
18.5	11 994.912	0.003				
19.5	11 994.120	− 0.002				
			Band IV (upper component)			
1.5					11 764.795	0.003
2.5			11 762.276	− 0.007	11 766.485	− 0.004
3.5	11 758.765	− 0.005	11 762.970	− 0.006	11 768.156	− 0.009
4.5	11 758.455	− 0.005	11 763.643	− 0.006	11 769.811	− 0.008
5.5	11 758.123	− 0.006	11 764.294	− 0.005	11 771.445	− 0.004
6.5	11 757.770	− 0.006	11 764.919	− 0.007	11 773.052	− 0.004
7.5	11 757.396	− 0.004	11 765.526	− 0.004	11 774.638	0.000
8.5	11 756.997	− 0.003	11 766.104	− 0.004	11 776.194	0.001
9.5	11 756.575	− 0.001	11 766.664	0.003	11 777.724	0.003
10.5	11 756.128	0.002	11 767.188	0.002	11 779.225	0.006
11.5	11 755.653	0.005	11 767.687	0.006	11 780.693	0.007
12.5	11 755.142	0.001	11 768.156	0.010	11 782.123	0.002
13.5	11 754.606	0.003	11 768.581	0.003		
14.5	11 754.035	0.002	11 768.971	− 0.005		
15.5	11 753.432	0.003	11 769.370	0.034		
16.5	11 752.790	0.002	11 769.633	− 0.025		
17.5	11 752.091	− 0.018				
			Band IV (lower component)			
1.5					11 760.206	0.002
2.5			11 757.698	0.003	11 760.377	0.004
3.5	11 754.187	0.005	11 756.863	0.002	11 760.529	0.006
4.5	11 752.349	0.004	11 756.010	0.003	11 760.659	0.005
5.5	11 750.497	0.009	11 755.139	0.005	11 760.771	0.005
6.5	11 748.617	0.006	11 754.249	0.006	11 760.862	0.003
7.5	11 746.720	0.003	11 753.338	0.005	11 760.938	0.004
8.5	11 744.806	0.003	11 752.407	0.002	11 760.994	0.002
9.5	11 742.874	0.002	11 751.460	0.001	11 761.031	− 0.001
10.5	11 740.926	0.002	11 750.497	0.000	11 761.053	− 0.003

TABLE I (*continued*).

	P		*Q*		*R*	
J"	Obs.	Obs. − Calc.	Obs.	Obs. − Calc.	Obs.	Obs. − Calc.
11.5	11 738.958	− 0.001	11 749.516	− 0.003	11 761.061	− 0.004
12.5	11 736.974	− 0.004	11 748.522	− 0.003		
13.5	11 734.976	− 0.006	11 747.510	− 0.006	11 761.031	− 0.007
14.5			11 746.488	− 0.006	11 760.998	− 0.007
15.5			11 745.454	− 0.004	11 760.953	− 0.006
16.5			11 744.406	− 0.005	11 760.900	− 0.003
17.5			11 743.351	− 0.002	11 760.836	0.000
18.5			11 742.284	− 0.001	11 760.763	0.002
19.5			11 741.209	0.000	11 760.679	0.001
20.5			11 740.134	0.008	11 760.591	0.002
21.5			11 739.049	0.013	11 760.504	0.010
22.5			11 737.950	0.008	11 760.401	0.004
23.5			11 736.848	0.003	11 760.289	− 0.008
24.5			11 735.739	− 0.008	11 760.192	− 0.005
			Band V (upper component)			
3.5			12 002.698	− 0.014		
4.5			12 003.400	− 0.003		
5.5			12 004.071	− 0.005		
6.5	11 997.570	− 0.011	12 004.728	− 0.002	12 012.860	0.002
7.5	11 997.234	− 0.002	12 005.364	− 0.001	12 014.474	0.003
8.5	11 996.870	− 0.002	12 005.977	− 0.002	12 016.066	0.003
9.5	11 996.486	− 0.001	12 006.574	0.003	12 017.635	0.004
10.5	11 996.083	0.002	12 007.145	0.004	12 019.178	0.003
11.5	11 995.655	0.004	12 007.692	0.006	12 020.693	0.000
12.5	11 995.203	0.006	12 008.203	− 0.001	12 022.177	− 0.005
13.5	11 994.720	0.003	12 008.697	0.002		
14.5	11 994.210	0.001	12 009.147	− 0.009		
			Band V (lower component)			
4.5	11 992.111	0.007	11 995.769	0.004		
5.5	11 990.272	0.002	11 994.912	− 0.004		
6.5	11 998.427	0.006	11 994.055	0.004	12 000.672	0.006
7.5	11 986.552	− 0.006	11 993.176	0.003	12 000.775	0.003
8.5	11 984.681	0.001	11 992.282	0.002	12 000.863	− 0.002
9.5	11 982.790	0.002	11 991.374	0.000	12 000.946	0.000
10.5	11 980.882	− 0.001	11 990.453	− 0.002	12 001.010	− 0.004
11.5	11 978.957	− 0.009	11 989.521	− 0.003	12 001.065	− 0.005
12.5	11 977.064	0.028	11 998.576	− 0.006	12 001.135	0.018
13.5	11 975.091	0.004	11 987.622	− 0.007		
14.5	11 973.139	− 0.005	11 986.659	− 0.008		
15.5			11 985.688	− 0.008		
16.5			11 984.719	0.002		
17.5			11 983.731	0.000		
18.5			11 982.737	− 0.003		
19.5			11 981.740	− 0.004		
20.5			11 980.753	0.008		

bands III, IV, and V, and their approximate locations are indicated in Fig. 1. The frequency region in the vicinity of band IV ($\sim$11 750 cm^{-1}) was relatively uncluttered, and nearly all the observed lines were in fact part of band IV. However, the spectrum was quite congested between 11 900 and 12 000 cm^{-1}, and less than half the lines could be assigned to bands III and V. This region is where autodetachment features for dipole-bound states might be expected, since transitions from the FeO^- ground state to the lowest lying $^5\Delta_4$ spin-orbit state of FeO are expected here.

The five assigned bands are briefly discussed below. The obtained line positions and calculated fits are listed in Table I.

A. Medium resolution data

(1) Band I, shown in Fig. 2, is a textbook case of well-resolved *P* and *R* branches separated by an unresolved *Q* branch. The *P* branch overlaps another band system at high *J*, and the *P*(33.5) and *R*(31.5) lines are perturbed, indicating an upper state perturbation. The lowest observed *P* and *R* branch transitions are the *P*(3.5) and *R*(2.5) lines, indicating that $\Omega = 2.5$ for both states. The observed intensity distribution, in which the *P* and *R* branches are of equal intensity and the *Q* branch is considerably weaker, is consistent with a $\Delta\Lambda = \Delta\Omega = 0$ transition. The transitions are

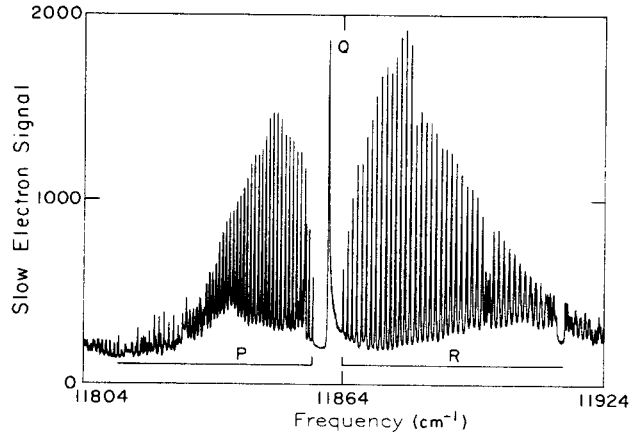

FIG. 2. Medium resolution ($\sim$1 GHz or 0.03 cm^{-1}) scan of the slow electron cross section in the 11 804–11 924 cm^{-1} frequency region (band I). The rotational spectrum is due to excitation of the $A\,^4\Delta_{5/2}$ valence state from the $X\,^4\Delta_{5/2}$ spin-orbit level in the FeO^- ground state, followed by autodetachment. Near $\sim$11 854 cm^{-1} an unidentified band system is present.

quite intense; the peak count rates are 100 kHz, while the total ion current is $\sim 10^9\ s^{-1}$.

(2) Band II, displayed in Fig. 3, is approximately an order of magnitude less intense than band I, and $R(9.5)$ is the first R branch line that can be clearly distinguished from the Q branch. The hump under the P branch is probably an unresolved Q branch from another band system. The $P(3.5)$ and $Q(3.5)$ lines are the first transition observed, so this is an $\Omega' = 2.5 \leftarrow \Omega'' = 3.5$ transition.

B. High resolution data

(1) The R branch of band III is shown in Fig. 4. A P branch of similar intensity occurs between 11 989 and 11 998 cm^{-1}. Both branches consist of several narrow lines with widths close to the instrumental resolution, followed by a series of lines with widths that increase rapidly with J. The lowest observed lines are the $R(13.5)$ and $P(15.5)$ transitions. This is not a reflection of Ω in either state, but is due instead to the fact that several rotational levels of the upper state for this band lie below the electron detachment threshold and do not autodetach (see below). Although transitions are observed near where the Q branch is expected, they are too weak and irregular to be assigned. Thus the Q branch is either very weak or nonexistent, implying $\Delta\Omega = 0$ for band III. The R branch in Fig. 4 shows effects from perturbations, and the lines from the perturbing state are indicated in the figure. Unfortunately, the P branch for band III, which also shows perturbations, occurs in a congested region of the spectrum and the perturbing lines could not be assigned.

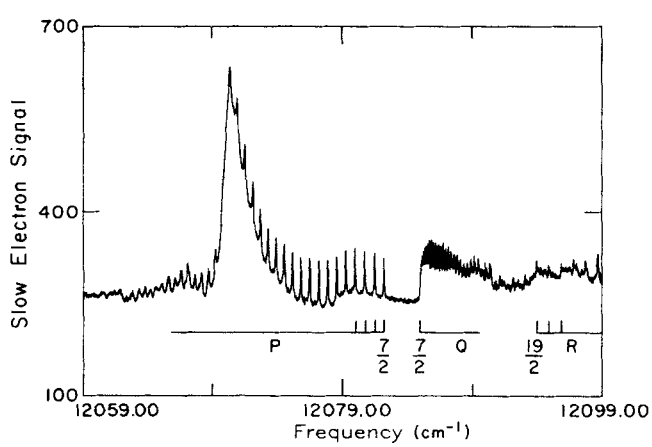

FIG. 3. Medium resolution ($\sim$1 GHz or 0.03 cm^{-1}) scan of the slow electron cross section in the 12 059–12 109 cm^{-1} frequency region (band II). The rotational spectrum is due to excitation of the $A\,^4\Delta_{5/2}$ valence state from the $X\,^4\Delta_{7/2}$ FeO^- ground state, followed by autodetachment. The P branch is superimposed upon an underlying unresolved structure peaking at $\sim$12 069 cm^{-1}.

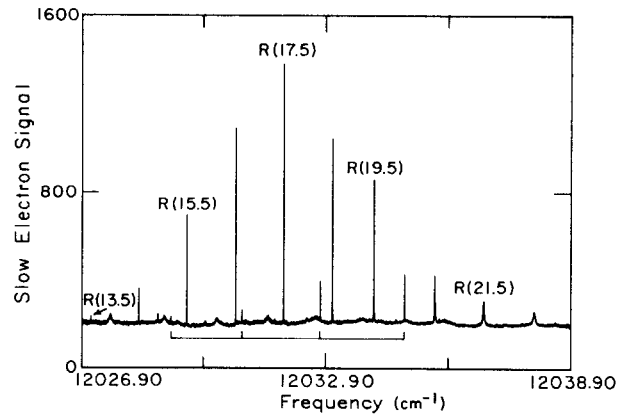

FIG. 4. High resolution ($\sim$20 MHz) of band III R branch. The R branch is perturbed near 12 034 cm^{-1}. Four lines assumed to belong to the perturbing system are marked below the experimental curve.

(2) In two frequency regions, near 11 761 cm^{-1} (band IV) and 12 000 cm^{-1} (band V), the same spectral pattern occurs over a range of $\sim$50 cm^{-1}. Analysis of these regions shows that each of these bands consists of two sub-bands each with a P, Q, and R branch. The intensity distribution in the two bands is about the same; in each band, $I_Q \cong I_P \cong 2I_R$ in the higher energy sub-band, and $I_Q \cong I_R \cong 2I_P$ in the lower sub-band. Based on the transitions with linewidths exceeding the Doppler width, the intensity of band V is about a factor of 5 less than band III, which lies in the same frequency region. The lower energy R branch in band IV is shown in Fig. 5. As in band III, the lowest J lines are very narrow, and

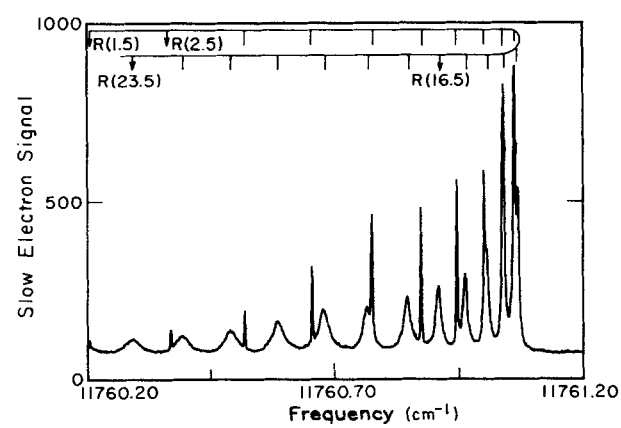

FIG. 5. High resolution ($\sim$20 MHz) scan of the R branch for the lower energy sub-band in band IV.

rapid broadening with increasing J is observed. The first observed lines in band IV indicate that both sub-bands are $\Omega' = 5/2 \leftarrow \Omega'' = 3/2$ transitions. Band V occurs in a more congested region, and the background from direct photodetachment is considerably larger because the laser frequency is higher. This makes it harder to pick out the lowest J lines which, as can be seen in Fig. 5, are quite low in intensity. The value of Ω for band V cannot be determined with confidence solely on the basis of the missing lines at low J.

IV. SPECTROSCOPIC ANALYSIS

The bands were assigned first with combination differences, and more precise constants were obtained by least-squares fitting to a rotational energy level expression. With the exception of the upper states for bands IV and V, the rotational levels in each band were adequately fit with the simple expression

$$E(J) = T_\Omega + B_\Omega J(J+1) - D_\Omega J^2(J+1)^2. \quad (1)$$

The identification of upper and lower states common to the various bands was done by assuming that electronic states with the same combination difference values and rotational constants are in fact the same state. In addition, in the cases where there appears to be a common upper state, the autodetachment linewidth dependence on J must be identical. This procedure shows that bands I and II have the same upper state ($\Omega' = 5/2$), bands II and III have the same lower state ($\Omega'' = 7/2$), bands I and V have the same lower state ($\Omega'' = 5/2$), and bands IV and V have the same upper state ($\Omega' = 5/2$). The energy ordering of the FeO^- electronic states determined by these linkages and their rotationless energy intervals relative to the FeO^- ground state are shown in Fig. 6. The states are labeled by their most likely term values (see below). Figures 7 and 8 show the autodetachment linewidths as a function of J for the three upper states. The widths were determined by fitting each line to a Lorentzian profile, a procedure which left no systematic residuals,

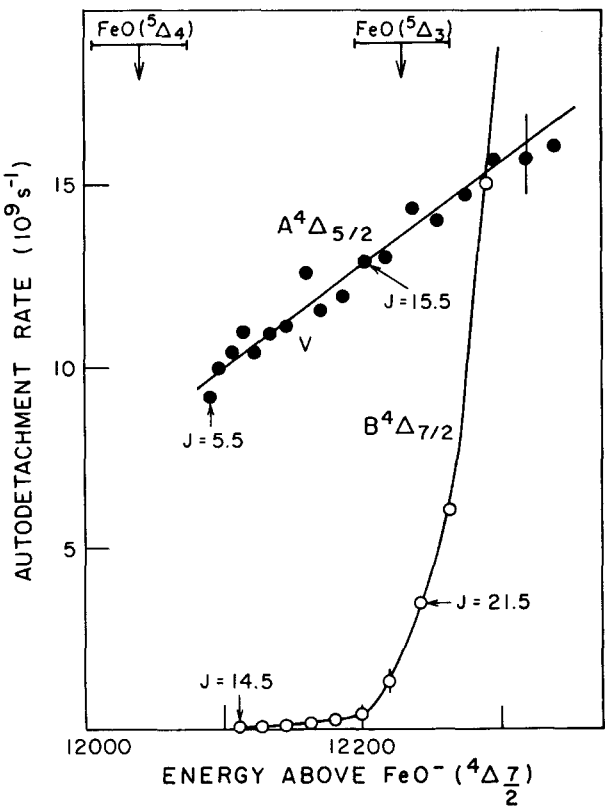

FIG. 7. Rotational dependence of the FeO^- autodetachment rates for the $A\,^4\Delta_{5/2}$ and $B\,^4\Delta_{7/2}$ states. The FeO ($^5\Delta_4$ and $^5\Delta_3$) thresholds are indicated.

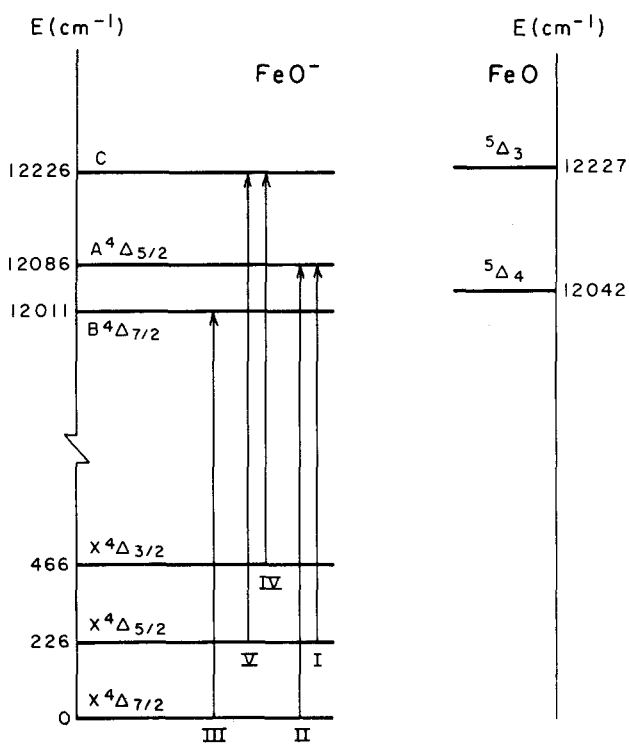

FIG. 6. Energy level diagram for FeO^- and FeO with the observed transitions and rotationless band intervals indicated.

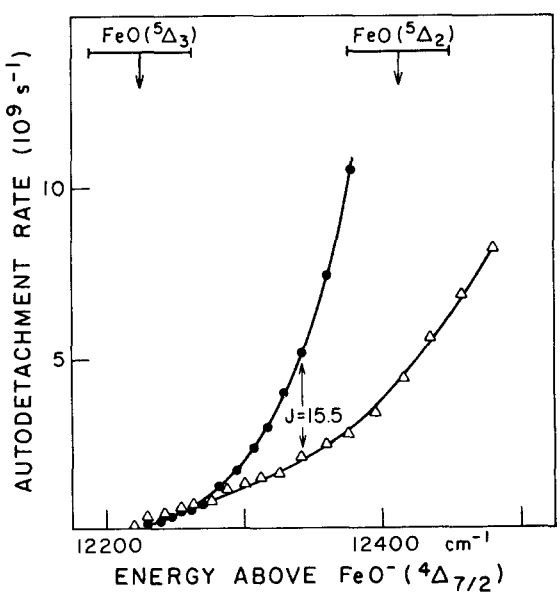

FIG. 8. Rotational dependence of the FeO^- autodetachment rates for the two components of the C state. Triangles represent the lower energy component. The FeO ($^5\Delta_3$ and $^5\Delta_2$) thresholds are indicated.

and confirms that these widths can be properly interpreted as autodetachment lifetimes.

The three observed lower electronic states are labeled by $\Omega'' = 3.5$, 2.5, and 1.5. The energy interval is about 230 cm^{-1}, and $\Omega'' = 3.5$ is the lowest in energy. This interval is close to the spin-orbit separation of 180 cm^{-1} between the $X\,^5\Delta$ multiplets in neutral FeO. Our results suggest that the three lower states are spin-orbit multiplets of the ground state of FeO^-, and the fact that $\Omega'' = 3.5$ is the lowest observed multiplet is consistent with the prediction of an inverted $X\,^4\Delta$ ground state for FeO^-. Fitting the energy intervals within the $X\,^4\Delta$ multiplet to the diagonal spin-orbit and spin–spin interaction terms,

$$A L_z S_z + 2\lambda/3(3S_z^2 - S^2), \tag{2}$$

we obtain $A = -119.9\ cm^{-1}$ and $\lambda = 3.39\ cm^{-1}$. For comparison, A and λ for the $X\,^5\Delta$ ground state of FeO are -94.9044 and $0.9049\ cm^{-1}$, respectively.[11]

The intensity distribution in band I indicates a $\Delta\Lambda = \Delta\Omega = 0$ transition, and based on this the upper state for this band is assigned as the $A\,^4\Delta_{5/2}$ state. This means that band II is the $A\,^4\Delta_{5/2} \leftarrow X\,^4\Delta_{7/2}$ transition, and the considerably lower intensity of this band relative to band I can be understood since it violates the Hund's case (a) $\Delta\Sigma = 0$ propensity rule. This violation means that there must be some spin-orbit mixing in either the A or X states. This is to be expected for molecules containing d electron atoms. While the vibrational numbering of the upper and lower states cannot be explicitly determined, the high intensity of band I, coupled with the similarity of rotational constants in the X and A states, strongly suggests we are dealing with a 0–0 vibrational transition.

The intensity distribution in band III indicates a $\Delta\Lambda = \Delta\Omega = 0$ transition, and the upper state for this band is labeled the $B\,^4\Delta_{7/2}$ state in Fig. 6. Again, we cannot explicitly determine the vibrational level of the B state. However, the autodetachment rate data indicate it is most likely the $v = 0$ level. This upper state is definitely not simply another spin-orbit multiplet of the $A\,^4\Delta$ manifold. The integrated intensity of even the most intense lines in band III is much less than the lines in band I, whereas if band III were the $A\,^4\Delta_{7/2} \leftarrow X\,^4\Delta_{7/2}$ transition, then the intensities should be comparable. In addition, the upper states in bands I and III are only $\sim 70\ cm^{-1}$ apart, and a splitting closer to 200 cm^{-1} would be expected if these were spin-orbit multiplets of the same $^4\Delta$ manifold. The differences between the two upper states are discussed in more detail in the next section. The large number of missing lines at low J for band III can be explained by the energy level diagram in Fig. 9. This shows the rotational energy levels for the $A\,^4\Delta_{5/2}$ and $B\,^4\Delta_{7/2}$ states, as well as the $X\,^5\Delta_4$ state of neutral FeO using an electron affinity of 12 042($\pm$40) cm^{-1}.[10(b)] All energies are referred to the $X\,^4\Delta_{7/2}\,FeO^-$ ($J = 7/2$) state. According to this diagram, the $B\,^4\Delta_{7/2}$ rotational levels with $J \leqslant 7.5$ lie below the detachment threshold. They therefore cannot autodetach and are not observed in our experiment. However, the next rotational levels lie above the threshold in Fig. 9, and the $J = 12.5$ level lies above the first two rotational levels of the $A\,^4\Delta_{5/2}$ state, so it certainly has enough energy to autodetach. These levels must detach by large ΔJ transitions, however, and autodetachment by this process may be too slow to be detected in our apparatus (see below).

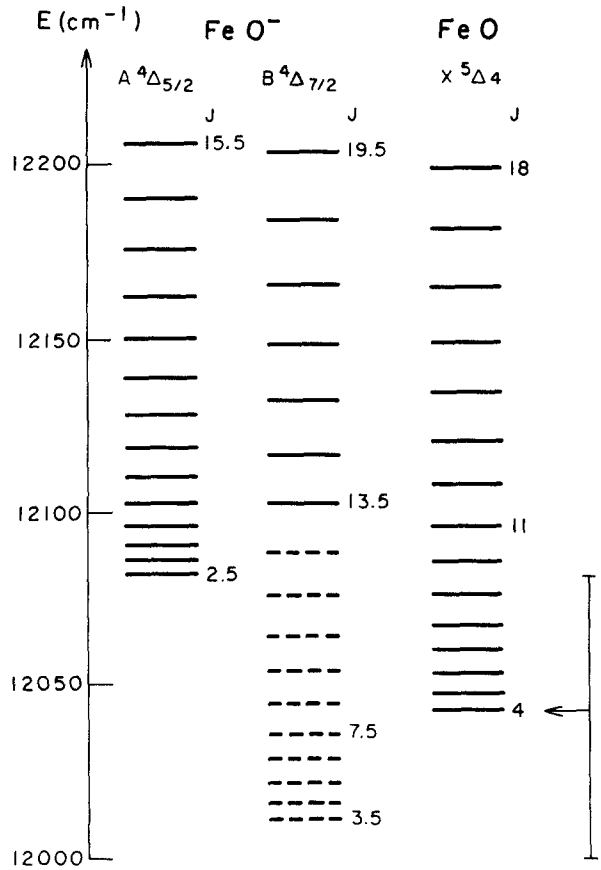

FIG. 9. Schematic representation of rotational levels for the $A\,^4\Delta_{5/2}$ and $B\,^4\Delta_{7/2}\,FeO^-$ states, and the $X\,^5\Delta_4$ FeO state. Solid lines represent observed levels, dashed lines unobserved levels. The solid bar at the right of the figure represents the uncertainty in the location of the FeO manifold with respect to that of FeO^-.

A similar line of reasoning indicates why the $A\,^4\Delta_{7/2} \leftarrow X\,^4\Delta_{7/2}$ transition is not observed. The $A\,^4\Delta_{7/2}$ state probably lies $\sim 200\ cm^{-1}$ below the observed $A\,^4\Delta_{5/2}$ state, which in turn lies $\sim 40(\pm 40)\ cm^{-1}$ above the detachment threshold. The $A\,^4\Delta_{7/2}$ state is therefore bound with respect to detachment by $\sim 160(\pm 40)\ cm^{-1}$, so its rotational levels with $J \lesssim 20$ cannot autodetach. The higher levels can only detach through unfavorably large ΔJ transitions and can easily go undetected.

One might also wonder why the higher energy spin-orbit multiplets in the A and B manifold are not observed. This could be due to another limitation of autodetachment spectroscopy: electronic states that lie well above the detachment threshold may autodetach so quickly that lifetime broadening obscures any rotational structure. For example, we believe that the broad, unresolved features under band I (see Fig. 1) are from the $A\,^4\Delta_{3/2} \leftarrow X\,^4\Delta_{3/2}$ band. The rotational spacing in these bands is typically 1 cm^{-1}, so autodetachment lifetimes less than 5 ps will result in an unresolved spectrum. Bands originating from the $X\,^4\Delta_{1/2}$ state access even more highly excited spin-orbit multiplets of the A and B manifold, and are even less likely to exhibit resolved struc-

TABLE II. Spectroscopic constants for the X, A, and B states of FeO^-. All units in cm^{-1}. The errors listed in parentheses are one standard deviation of a least-squares fit using expressions given in the text. All term energies are relative to the $X\,^4\Delta_{7/2}$ state.

	T	B	D
$X\,^4\Delta_{7/2}$	0	0.4972(2)	$9(4)\times10^{-7}$
$X\,^4\Delta_{5/2}$	226.123(7)	0.4997(3)	$8(4)\times10^{-7}$
$X\,^4\Delta_{3/2}$	465.82(1)	0.5018(1)	$7(2)\times10^{-7}$
$A\,^4\Delta_{5/2}$	12 086.00(8)	0.5045(2)	$1.3(4)\times10^{-6}$
$B\,^4\Delta_{7/2}$	12 011.19(5)	0.5046(4)	$3.6(7)\times10^{-6}$

ture. The constants obtained for the X, A, and B states are shown in Table II.

The common upper state in bands IV and V could not be fit using the simple energy expression (1). After some trial and error, the higher and lower energy sub-bands were fit using Eqs. (3) and (4), respectively, for the upper state energy levels

$$E(J) = T + B(J+1/2)(J+3/2) - (D+\Delta D)(J+1/2)^2(J+3/2)^2 + 1/2p(J+3/2), \quad (3)$$

$$E(J) = T + B(J-1/2)(J+1/2) - (D-\Delta D)(J+1/2)^2(J-1/2)^2 - 1/2p(J-1/2). \quad (4)$$

The fit was not significantly improved by allowing different values of B or p for each sub-band, or by adding a term proportional to J^3. However, the use of different effective centrifugal distortion constants ($D \pm \Delta D$) for the two sub-bands reduced the residual standard deviation by an order of magnitude. The constants for the upper state, designated the C state, are displayed in Table III. The quantity ΔD is not small; as Table III shows, $\Delta D/D \approx 2$.

Expressions (3) and (4) are similar to the energy level formulas for a $^2\Sigma$ state in which the parameter p includes the spin-rotation splitting and spin-doubling effects from a nearby $^2\Pi$ state.[19] A $^2\Sigma \leftarrow {}^4\Delta$ transition can be ruled out because $\Omega' = 2.5$ for the upper state, but Eqs. (3) and (4) suggest that this state can be thought of as a σ electron weakly coupled to a neutral FeO core, with nonzero Ω. The rotational energy of the core is $BN(N+1)$, where $N = J \pm 1/2$ depending on whether the projection of the σ electron on the internuclear axis is $\mp 1/2$. However, since p is comparable to B, it seems that conventional perturbation treatments may be inadequate to describe the upper states. The physical significance of the parameter ΔD is unclear at this time. Finally, it is not obvious why the intensity distributions in bands IV and V are nearly identical even though the lower states in the two bands have different values of Ω. In short, while the C state can be fit by simple energy expressions, we have a poor understanding of its nature.

TABLE III. Spectroscopic constants for C state of FeO^-, using band IV. All units in cm^{-1}. As in Table II, T is the term energy referenced to the $X\,^4\Delta_{7/2}$ state. The other quantities are defined in Eqs. (3) and (4).

T	12 225.50(1)
B	0.4918(2)
p	0.5458(4)
D	$2.2(4)\times10^{-6}$
ΔD	$4.25(4)\times10^{-6}$

V. DISCUSSION

The spectroscopic results are best understood by considering the molecular orbital configurations for FeO and FeO^-. These have been investigated recently in a CI calculation by Krauss and Stevens.[9] Although multiconfiguration effects are expected to play a large role in both species, for the purposes of discussion it is convenient to describe the various electronic states by the dominant single configuration. For the $^5\Delta$ ground state of neutral FeO, this configuration is $\delta^3\pi_a^2\,\sigma_l\,\pi_b^4\,\sigma_b^2$, where π_b is a slightly bonding orbital localized on the O atom, σ_b is a bonding orbital, π_a is an antibonding orbital resulting from the Fe $d\pi$–O$p\pi$ interaction, and δ and σ_l are nonbonding orbitals on the Fe atom. A more detailed description of these orbitals can be found in Ref. 9. The rotational constants for the ground state of FeO^- are similar to those for the ground state of FeO, so one can reasonably assume that the ground state of FeO^- is formed by the addition of an electron to either the δ or σ_l nonbonding orbitals, yielding a $^4\Sigma^-$ state or a $^4\Delta$ state, respectively. The observed $\Omega = 7/2$ ground state rules out a $^4\Sigma^-$ state, so this simple molecular orbital picture combined with our results supports the $^4\Delta$ state as the FeO^- ground state.

Bands I, II, and III are most likely $\sigma^* \leftarrow \sigma_l$ transitions, and again, since the rotational constant changes only slightly between the upper and lower states, the upper σ^* orbital appears to be largely nonbonding for these bands. We note, for comparison, that the $^5\Phi \leftarrow X\,^5\Delta$ transition in neutral FeO, in which a bonding Π_b electron is excited into the σ_l orbital, results in a substantial change in the rotational constant from 0.5168 cm^{-1} in the $X\,^5\Delta$ state to $\sim$0.450 cm^{-1} in the $^5\Phi$ state.[11] In any case, the two upper states for the three FeO^- bands can be thought of as a $^5\Delta$ neutral FeO core plus a weakly bound σ^* electron. The core value Ω_c is related to Ω for the anion state in question by $\Omega_c = \Omega \pm 1/2$. Thus $\Omega_c = 4$ or 3 for the $B\,^4\Delta_{7/2}$ state. However, the autodetachment data suggest that $\Omega_c = 3$ for the $A\,^4\Delta_{5/2}$ state. It should be emphasized that the widely different intensities for band I and band III mean that the σ^* orbitals are not at all alike in the two upper states. In addition, the autodetachment rate data show that the interaction between the FeO core and σ^* electron is different for the upper states. We now explore this interaction by considering possible autodetachment mechanisms in FeO^-.

The various mechanisms responsible for autodetachment and autoionization, the analogous process in neutrals, have been discussed previously.[20–23] These mechanisms all have their origin in the breakdown of the Born–Oppenheimer approximation. That is, the autodetaching anion state is coupled to the (neutral + e^-) continuum by electronic, vibrational, or rotational terms in the molecular Hamiltonian which are usually neglected in constructing the adiaba-

tic potential energy curves for the anion and neutral electronic states. The mechanisms previously observed in negative ions have been vibrational and rotational autodetachment,[1,3–5] in which an internally excited ion undergoes a vibrational or rotational deexcitation, and the energy thereby released results in electron ejection.

In FeO^-, another possibility arises because spin-orbit excitation in the ion can also result in autodetachment. This is most likely to be the autodetachment mechanism for the $A\,^4\Delta_{5/2}$ state. The autodetachment rate is quite high ($\sim 10^{10}$ s^{-1}), even for the lowest values of J and it slowly increases with J. This behavior is similar to the vibrational autodetachment previously observed in excited valence states of C_2^-. In the present case, however, we are most likely in the $v=0$ level of the $A\,^4\Delta_{5/2}$ state, and the internal excitation available for autodetachment is the spin-orbit excitation of the neutral FeO core, either the $^5\Delta_3$ or $^5\Delta_2$ state. The conversion of the $^5\Delta_3$ core to the $^5\Delta_4$ core by a "spin flip" of one of the core electrons will release 180 cm^{-1} of energy, which is enough to autodetach any of the anion rotational energy levels to $FeO(^5\Delta_4) + e^-$ products. This mechanism is analogous to the autoionization of Rydberg states of Ar atoms,[23] in which the Rydberg states converging to the spin-orbit excited $Ar^+(^2P_{1/2})$ limit can autoionize to $Ar^+(^2P_{3/2}) + e^-$. On the other hand, if the $A\,^4\Delta_{5/2}$ state had a $^5\Delta_2$ core, two spin flips of core electrons would be necessary to autodetach to $FeO(^5\Delta_4) + e^-$, which is the only available product channel for $J \lesssim 20$. It seems that such a product of two weak nonadiabatic terms would result in a much slower autodetachment rate than we observe. Thus we claim that the $A\,^4\Delta_{5/2}$ state does have a $^5\Delta_3$ core. Spin-orbit autoionization of HI has very recently been observed, although individual rotational levels were not resolved.[24]

The autodetachment rate for the $B\,^4\Delta_{7/2}$ state shows a dramatically different functional dependence on J than is seen for the $A\,^4\Delta_{5/2}$ state. The rate is very slow for the first few observed rotational levels, and then rises rapidly above $J = 20.5$. A similar dependence on J has been observed in rotational autodetachment of dipole-bound states in $C_2H_3O^-$ [4] and CH_2CN^-.[5] If the FeO core for the $B\,^4\Delta_{7/2}$ state is $^5\Delta_4$ ($v=0$), then rotational autodetachment is the *only* autodetachment decay mechanism available to the anion. That is, rotationally excited levels of the $B\,^4\Delta_{7/2}$ state that lie above the detachment threshold can decay to $FeO(^5\Delta_4) + e^-$ by the conversion of rotational energy and angular momentum J into energy and orbital angular momentum l of the outgoing electron. If there were a $^5\Delta_3$ core for the ion state, a spin-flip would be required in addition to a ΔJ of the rotating core, and for the same reasons given above, a $^5\Delta_4$ core is more likely. However, Russek[25] has introduced an internal conversion formalism for autodetachment from $B\,^4\Delta_{7/2}$ using a $^5\Delta_3$ core and obtains qualitatively correct autodetachment rates.

The observed autodetachment rates for the $B\,^4\Delta_{7/2}$ state can be understood by considering the autodetachment transitions available to the various rotational energy levels for this state. Assuming the energy level diagram in Fig. 9 is correct, the first rotational level of the $B\,^4\Delta_{7/2}$ state that can autodetach is the $J = 8.5$ level. However, this can only detach by a $\Delta J = -4.5$ transition with the resulting ejection of an $l = 4$ or 5 electron. This will be an *extremely* slow process because of the large centrifugal barrier for an electron with such high orbital angular momentum. If the autodetachment lifetime exceeds the transit time through the interaction region of the apparatus (~ 2 μs) or the fluorescence lifetime of the excited state, then the autodetachment signal will be severely attenuated and may not be observed at all. This is the most likely explanation for the missing autodetachment transitions between $J = 8.5$ and 13.5 in the $B\,^4\Delta_{7/2}$ state. On the other hand, higher rotational levels of this state can autodetach via ejection of lower angular momentum electrons. The $J = 13.5$ level, which is the first one observed, can autodetach by ejecting an $l = 2$ or 3 electron. At $J = 19.5$, where the autodetachment rate increases sharply, an $l = 1$ or 2 electrons can be ejected. The exact nature of the available autodetachment transitions is quite sensitive to the FeO electron affinity, which currently has error bars of ± 40 cm^{-1}. Nonetheless, the correlation of the rapid increase in autodetachment rate with the accessibility of small ΔJ transitions appears to work for this system and for CH_2CN^- and $C_2H_3O^-$ as well.

The next issue to address is whether one can clearly distinguish between valence and dipole-bound states of negative ions if the electron binding energies are comparable. The temptation in FeO^- is to claim that the $B\,^4\Delta_{7/2}$ state is dipole bound because its autodetachment rate behavior mirrors that of known dipole-bound states, and that the $A\,^4\Delta_{5/2}$ state is a valence state because of its similarity to the C_2^- autodetaching valence states.

The assignment of $A\,^4\Delta_{5/2}$ as a valence state is the more tenuous claim. It is possible that the $A\,^4\Delta_{5/2}$ state is a dipole-bound state with a spin-orbit excited core, and that the autodetachment rates for this state simple reflect the fact that spin-orbit coupling to the continuum, when it is a viable mechanism, overwhelms rotational autodetachment. The fact that spin-orbit autoionization is quite rapid for high Rydberg states of atoms suggests that it is also a reasonably facile mechanism for dipole-bound states. One could argue that because the rapid increase in autodetachment rate at high J is not observed, the $A\,^4\Delta_{5/2}$ state is not a dipole-bound state. However, pure rotational autodetachment from this state results in $FeO(^5\Delta_3) + e^-$, and the $A\,^4\Delta_{5/2}$ state is bound by ~ 140 cm^{-1} with respect to this channel. This means that the $J = 40$ level, which was the highest observed, most rotationally autodetach by a $\Delta J = -4.5$ transition, and the contribution from this process should be negligible. One obviously cannot rule out rotational autodetachment dominating at much higher values of J, for which no transitions were seen. A strong argument for classifying the A state as a valence state relates to its binding energy. The lowest energy $A\,^4\Delta_{7/2}$ multiplet which, as discussed previously, is not observed, should be bound by ~ 140 cm^{-1} with respect to electron detachment. This is a high binding energy for a dipole-bound state in which the dipole moment of the core, while not yet measured experimentally, is calculated to be 3.2 D. For comparison, the dipole moment of acetaldehyde enolate radical is calculated to be 3.54[8] and 3.191 D,[26] and the dipole-bound electron is bound by only ~ 5 cm^{-1}.[4]

The claim that the autodetachment rates of the $B\,^4\Delta_{7/2}$ state are a signature of a dipole-bound state can be made with more confidence. The rotational–electronic coupling that leads to rotational autodetachment is expected to be extremely important in a dipole-bound state. The orbital for a weakly dipole-bound electron typically extends well over 10 Å.[7] If the molecule is rotating, this diffuse orbital must track the rotation of the neutral molecular core, because otherwise the anisotropic dipolar field will be averaged out.[27] This means that far from the molecular core, where the electron has very low kinetic energy in the nonrotating molecule, a significant fraction of the electronic velocity is due to the rotation of the molecule. This is exactly the situation in which nonadiabatic coupling between two degrees of freedom (electronic and rotational) becomes important, so it is not surprising that, once centrifugal barrier effects can be overcome, the autodetachment rate increases rapidly with J for dipole-bound states. We note that based on these considerations, rotational autoionization in Rydberg states should not show a strong dependence on J, because Rydberg electrons do not have to track molecular rotation. Indeed, the theoretical treatment of Rydberg states[23] shows that the rotational autoionization rate is virtually independent of J. This further supports the idea that the autodetachment rates seen for the $B\,^4\Delta_{7/2}$ state do not occur just because rotational autodetachment is the only possible decay mechanism, but rather because of the rotational–electronic coupling unique to a dipole-bound state. The identification of this state as a dipole-bound state almost certainly means that the observed transitions populate the $v = 0$ state. If the transitions were to the $v = 1$ state, the $v = 0$ state would be bound by ~ 700 cm^{-1}, a quantity which is unreasonably large.

We conclude with some remarks on the autodetachment rates for the C state. The rise in the autodetachment rate with J resembles that of the $B\,^4\Delta_{7/2}$ state, although it is less abrupt for both subbands. At this point, all that can be said is that this looks like a dipole-bound state in which the neutral core is a very low-lying electronic state of FeO. Merer has recently observed such a low-lying electronic state,[28] although its band origin and term symbol are unknown. The details of the autodetachment mechanism for the C state will have to wait until its spectroscopy is better understood.[29]

VI. SUMMARY

The anion FeO^- shows the richest electronic state structure of any negative ion studied to date. The ground state is most likely an inverted $^4\Delta$ state, and three electronic states lying near the detachment threshold have been identified and rotationally assigned. The dependence of the autodetachment rate on rotation for these states suggests that two are dipole-bound states, and the third may be a valance excited state that can be described in terms of conventional molecular orbitals. It would be most interesting to photodetach other transition metal oxide anions near their detachment thresholds to see how universal this complex electronic structure is in this type of ion.

ACKNOWLEDGMENTS

This work was supported by the National Science Foundation under Grant Nos. CHE83-16628 and PHY86-04504. TA thanks the Danish Natural Science Council for a travel grant.

[1] D. M. Neumark, K. R. Lykke, T. Andersen, and W. C. Lineberger, J. Chem. Phys. **83**, 4364 (1985).
[2] N. H. Rosenbaum, J. C. Owrutsky, L. M. Tack, and R. J. Saykally, J. Chem. Phys. **84**, 5308 (1986); K. Kawaguchi and E. Hirota, *ibid.* **84**, 2953 (1986); B. D. Rehfuss, M. W. Crofton, and T. Oka, *ibid.* **85**, 1785 (1986); L. M. Tack, N. H. Rosenbaum, J. C. Owrutsky, and R. J. Saykally, *ibid.* **84**, 7056 (1986).
[3] G. Herzberg and A. Lagerqvist, Can. J. Phys. **46**, 2363 (1968); W. C. Lineberger and T. A. Patterson, Chem. Phys. Lett. **13**, 40 (1972); U. Hefter, R. D. Mead, P. A. Schulz, and W. C. Lineberger, Phys. Rev. A **28**, 1429 (1983).
[4] R. D. Mead, K. R. Lykke, W. C. Lineberger, J. Marks, and J. I. Brauman, J. Chem. Phys. **81**, 4883 (1984); K. R. Lykke, R. D. Mead, and W. C. Lineberger, Phys. Rev. Lett. **52**, 2221 (1984).
[5] K. R. Lykke, D. M. Neumark, T. Andersen, V. J. Trapa, and W. C. Lineberger, in *Laser Spectroscopy VII*, edited by Y. R. Shen and T. W. Hänsch (Springer, Berlin, 1985), pp. 130–133.
[6] W. R. Garrett, Phys. Rev. A **3**, 961 (1971).
[7] K. D. Jordan and W. Luken, J. Chem. Phys. **64**, 2760 (1976).
[8] R. W. Wetmore, H. F. Schaefer III, P. C. Hiberty, and J. I. Brauman, J. Am. Chem. Soc. **102**, 5470 (1980).
[9] M. Krauss and W. J. Stevens, J. Chem. Phys. **82**, 5584 (1985).
[10] P. C. Engelking and W. C. Lineberger, J. Chem. Phys. **66**, 5054 (1977); D. G. Leopold, K. K. Murray, and W. C. Lineberger (unpublished results).
[11] A. S-C. Cheung, A. M. Lyyra, A. J. Merer, and A. W. Taylor, J. Mol. Spectrosc. **102**, 224 (1983); A. S-C. Cheung, N. Lee, A. M. Lyyra, A. J. Merer, and A. W. Taylor, *ibid.* **95**, 213 (1982).
[12] W. H. Hocking, M. C. L. Gerry, and A. J. Merer, Can. J. Phys. **57**, 54 (1979); R. M. Gordon and A. J. Merer, *ibid.* **58**, 642 (1980); A. S-C. Cheung, A. W. Taylor, and A. J. Merer, J. Mol. Spectrosc. **92**, 391 (1982); A. S-C. Cheung, W. Zyrnicki, and A. J. Merer, *ibid.* **104**, 315 (1984).
[13] R. D. Mead, Ph.D. thesis, University of Colorado, Boulder, 1984.
[14] W. A. Goddard III (unpublished results).
[15] T. Andersen, K. R. Lykke, D. M. Neumark, and W. C. Lineberger, in *Electronic and Atomic Collisions*, edited by D. C. Lorents, W. E. Meyerhof, and J. R. Peterson (Elsevier, Amsterdam, 1986), pp. 791–798.
[16] D. M. Neumark, K. R. Lykke, T. Andersen, and W. C. Lineberger, Phys. Rev. A **32**, 1890 (1985).
[17] S. A. Lee and J. L. Hall, Appl. Phys. Lett. **25**, 367 (1976).
[18] R. Balhorn, H. Kunzmann, and F. Lebowsky, Appl. Opt. **11**, 742 (1972).
[19] R. N. Zare, A. L. Schmeltekopf, W. J. Harrop, and D. L. Albritton, J. Mol. Spectrosc. **46**, 37 (1973).
[20] R. S. Berry, J. Chem. Phys. **45**, 1228 (1966).
[21] J. Simons, J. Am. Chem. Soc. **103**, 3971 (1981); P. K. Acharya, R. A. Kendall, and J. Simons, *ibid.* **106**, 3402 (1984).
[22] J. Berkowitz, *Photoabsorption, Photoionization, and Photoelectron Spectroscopy* (Academic, New York, 1979), pp. 32, 33, 176–183.
[23] H. Lefebvre-Brion and R. W. Field, *Perturbations in the Spectra of Diatomic Molecules* (Academic, New York, 1986), pp. 392–396.
[24] T. A. Carlson, P. Gerard, M. O. Krause, G. Von Wald, J. W. Taylor, and F. A. Grimm, J. Chem. Phys. **84**, 4755 (1986).
[25] A. Russek, J. Chem. Phys. (submitted).
[26] E. S. Huyser, D. Feller, W. T. Borden, and E. R. Davidson, J. Am. Chem. Soc. **104**, 2956 (1982).
[27] For a symmetric top or a diatomic molecule with $\Lambda \geqslant 1$, the dipolar field is largely (but not completely) averaged out at high values of J.
[28] A. W. Taylor, A. S-C. Cheung, and A. J. Merer, J. Mol. Spectrosc. **113**, 487 (1985).
[29] A referee has pointed out that the C state could be $^6\Sigma_{5/2}$. This would explain the unusual rotational structure in the branches described. However, the lack of other analyzed rotational branches that could be ascribed to a $^6\Sigma$ state precludes a definitive assignment at this time.